Eurasia Journal of Science and Technology
ISSN: 2663-1016
DOI: https://doi.org/10.61784/ejst3074

MATCHING CONTROL STRATEGY FOR HYDROGEN CIRCULATION SYSTEM FOR ON-BOARD FUEL CELLS

JianHua Liu[1*], Jun Li[1], JingGuang Xie[1], NanNan Liao[1], YaNan Gao[2]
[1]*CRRC QISHUYAN CO., LTD, Changzhou, 213000, Jiangsu, China.*
[2]*Dept.of Economic Research, CRRC Academy Co., Ltd, Beijing 100070, China.*
Corresponding Author: JianHua Liu, Email: liujianhua.qj@crrcgc.cc

Abstract: A fuel cell hydrogen recirculation system improves hydrogen utilization by circulating hydrogen from the fuel cell anode outlet to the inlet. First, by analyzing the flow rate and pressure demand of fuel cell hydrogen circulation, the model of hydrogen circulation pump is determined and the demand allocation between the inducer and the hydrogen circulation pump is carried out. Based on the one-dimensional design theory of the ejector, a one-dimensional model of the ejector is established, and by fitting the flow-pressure rise curves of the ejector and the hydrogen circulating pump, the pressures, flow rates, and cycle ratios are calculated under the two arrangement schemes of series and parallel connection, and the corresponding matching strategies are formulated. By comparing the performance of the two schemes in series and parallel with the corresponding matching strategy, the arrangement scheme of the ejector and hydrogen circulation pump is determined.
Keywords: Fuel cells; Hydrogen recirculation system; Pilot injector; Hydrogen recirculation pumps

1 INTRODUCTION

Proton Exchange Membrane Fuel Cell (PEMFC), as a key carrier for hydrogen energy utilization, provides a reaction site for hydrogen and oxygen to convert chemical energy into electrical energy, which has the advantages of clean and efficient, stable operation, fast start-up, and faster response to load demand [1], and it is the most likely replacement of internal combustion engine in future One of the energy devices [2].

Since the PEMFC anode outlet contains hydrogen that is not involved in the reaction, if it is directly discharged, it will cause environmental pollution and even safety hazards, as well as wasting energy and increasing the cost of use [3]. In recent years, the method of recycling hydrogen from the anode outlet to the inlet for secondary hydrogen utilization using a recycling device has been widely studied and tested in order to improve fuel economy. However, the traditional single-component hydrogen recycling scheme is not mature enough for fuel cells, which mainly includes the following two aspects: first, the single pilot scheme, which has good hydrogen recycling capability in the operating zone where the output power of the electric pile is higher than 50% of the maximum power, but has poor pilot performance in the operating zone below 50% of the maximum power [4]; second, the single hydrogen recycling pump scheme, which can adjust the rotational speed according to the power of the electric pile to control the amount of hydrogen circulation, which can satisfy the circulation demand under full operating conditions, but at the same time, it will generate large parasitic power.

There are usually three schemes for fuel cell anode tail gas treatment: circulation mode, dead-end mode, and recirculation mode [5]. In the circulation mode, the gas from the anode outlet is directly discharged into the atmosphere; this scheme has a simple structure and low system cost, but the hydrogen is not fully utilized and a humidifier is required to humidify the inlet hydrogen to prevent membrane drying. In the dead-end mode, the exhaust valve is normally closed to prolong the residence time of hydrogen in the stack and thus improve the hydrogen utilization, but the nitrogen and water permeating from the cathode across the membrane to the anode may cover the three-phase reaction surface of the catalytic layer, resulting in a localized shortage of hydrogen at the anode, which leads to a reduction in the output power of the stack [6]. The recirculation mode uses a recirculation device to transport the hydrogen from the anode outlet to the anode inlet to participate in the reaction again, and since the anode exhaust gas contains water vapor generated by the electrochemical reaction and residual hydrogen, the recirculation process not only effectively improves the hydrogen utilization rate, but also has a certain humidification effect on the hydrogen at the anode inlet, which increases the effective utilization of the water of the fuel cell product, and this mode is the most widely used in fuel cell vehicles. This mode is the most widely used exhaust gas treatment method in fuel cell vehicles.

At present, the main two commonly used hydrogen circulation elements are the elicitor and the hydrogen circulation pump. Hydrogen circulation schemes mainly include: single elicitor, single hydrogen circulation pump, two-stage elicitor in parallel, elicitor and hydrogen circulation pump used in combination, and so on.

The research on the fuel cell system-based elicitor mainly focuses on the matching problem between the elicitor and the PEMFC system, including: the influence of the elicitor structure on the PEMFC system; the performance study of the elicitor under different operating parameters; the elicitor modelling method based on the PEMFC system, etc. Bao et al [7] established a dynamic model of the PEMFC system including elicitor and investigated the effect of the current on the performance of the elicitor by simulation, and the results showed that the elicitation ratio decreased abruptly when the current was instantaneously reduced and then increased rapidly. The effect of the current on the performance of the elicitor is investigated through simulation, and the results show that the elicitor ratio plummets to 0 and then rises back quickly when the current decreases instantaneously. Dadvar et al [8] investigated the correlation between the design

parameters of the stack and the design parameters of the elicitor, and by analyzing the effects of the activation area of the cell, the number of single cells, the diameter of the nozzle, and the diameter of the mixing chamber on the output efficiency of the fuel cell and the value of the current density corresponding to the maximum increment in efficiency, and based on this two dimensionless parameters, size ratio and diameter ratio, were proposed to establish a link between the design of the electric stack and the design of the inducer. MA et al [9] investigated the matching design problem between the inducer and the PEMFC system, quantified the actual boundary conditions of the inducer in the overall operating range, and established the design of the inducer including the cycle ratio, the hydrogen cycle ratio, the minimum current when the hydrogen cycle ratio is greater than 1.5, and the secondary current when the secondary current is wet and dry A comprehensive elicitor performance evaluation system has been developed that includes four metrics: circulation ratio, hydrogen circulation ratio, minimum current at hydrogen circulation ratio greater than 1.5, and ratio of hydrogen circulation ratio at wetting and drying of secondary stream.

For hydrogen circulation pumps are currently divided into two main categories: volumetric and vane. Among them, Roots-type, claw-type, and scroll-type are volumetric pumps, while vortex-type are vane pumps [10]. Roots-type pumps have a double-rotor structure, with the main and driven shafts parallel, and compress the gaseous medium through the rotary motion of the cam rotor. Roots-type pumps have higher pressure rise, smooth operation, low noise, low vibration, and no internal oil lubrication is required, which avoids contamination of the system by oil vapor. Claw type hydrogen circulation pump has two claw rotors rotating in opposite directions, the two rotors will not contact each other, and there is a very small gap between the rotor and the chamber shell. Claw pumps are stable, but have poor sealing, vibration and noise. Vortex pumps are mainly composed of fixed and driven two vortex discs. When driving the scroll disc rotation, the gas from the outer edge of the inhalation and compression between the two scroll discs and transported to the center of the scroll disc. Because of the small clearance within the scroll pump, there is less gas leakage, lower vibration and noise, but the pressure rise and flow rate of this type of pump is also smaller. The vane pump converts the mechanical energy of the vane into the kinetic energy of the fluid through the rotation of the impeller. Vane pumps are simple in structure, smaller in size and produce less energy consumption. The energy consumption and noise problems of hydrogen circulation pumps are the main reasons for limiting their use. He Lingxuan [11] established an energy consumption model for hydrogen circulation pumps for research, and the results showed that the energy loss of hydrogen circulation pumps is about 23.3% of the loss of fuel cell appurtenant equipment.

The combination of the pilot and the hydrogen circulation pump as the hydrogen circulation device of the PEMFC system can ensure the circulation demand at a very low power and can play a better performance for the scenario of frequent load change. When the fuel cell is in the low power zone, the ejector performance is not good, then the hydrogen circulation pump is activated to circulate hydrogen, when in the high-power zone, the ejector as the main circulation device can meet the demand. This scheme not only avoids the problem of poor performance of the pilot in the low power region, but also reduces the power consumed by the hydrogen circulation pump.

The combination of the pilot and the hydrogen circulation pump as the hydrogen circulation device of the PEMFC system can ensure the circulation demand at a very low power and can play a better performance for the scenario of frequent load change. When the fuel cell is in the low power zone, the ejector performance is not good, then the hydrogen circulation pump is activated to circulate hydrogen, when in the high-power zone, the ejector as the main circulation device can meet the demand. This scheme not only avoids the problem of poor performance of the ejector in the low-power region, but also reduces the power consumed by the hydrogen circulation pump. However, at this stage, the matching control strategy of the ejector and hydrogen circulation pump under on-board operating conditions needs to be further investigated. Therefore, based on the automotive fuel cell system, this paper designs a hydrogen recirculation system to meet its operational requirements. Finally, the matching control strategy of the hydrogen circulation subsystem is established for different operating conditions of the vehicle fuel cell.

2 DEMAND ALLOCATION FOR EJECTORS AND HYDROGEN CIRCULATION PUMPS

2.1 Fuel Cell Hydrogen Cycle System Structure

The design of hydrogen circulation system for on-board fuel cell puts higher requirements on the circulation volume under the whole power range and power loss. The traditional single ejector or hydrogen circulation pump can no longer meet the demand of the electric stack cycle, so this paper improves the hydrogen system structure of the on-board fuel cell system, adopting a combination of ejectors and hydrogen circulation pumps, the structural principle of the hydrogen circulation system is shown in Figure 1.

Hydrogen released from the high-pressure hydrogen storage cylinder enters the inlet of the hydrogen recycling device, i.e. the primary inflow port of the ejector, after the pressure is adjusted by the pressure reducing valve and the proportional valve; after the anode tail gas passes through the water separator, a part of the gas and the liquid water are discharged through the drainage and exhaust solenoid valve periodically, and a part of the gas enters the secondary inflow port of the ejector or the hydrogen recycling pump, and then it mixes with the new hydrogen and enters into the fuel cell to participate in the electrochemical reaction again. As the hydrogen demand of the stack is different under different working conditions, the corresponding flow resistance is also different. Therefore, the design of hydrogen circulation system should meet the demand of hydrogen circulation flow on the one hand, and the pressure demand on the other hand.

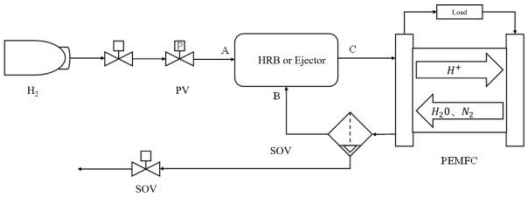

Figure 1 Schematic Diagram of Fuel Cell Hydrogen System

2.2 Hydrogen Cycle Flow Requirements

In fuel cell systems, in order to ensure that the hydrogen supply is sufficient and there is no shortage of reactants when the load changes suddenly, the hydrogen supplied to the anode of the fuel cell is generally in excess, and the actual flow rate of hydrogen is about 1.1 to 1.5 times of the theoretical flow rate [12, 13]. The volume flow rates of fresh hydrogen and circulating hydrogen as well as the molar fractions (volume fractions) of each component in the circulating gas in the 100kW fuel cell system at various currents were measured as shown in Table 1.

Table 1 Hydrogen Cycle Flow Requirements for Electric Stack

Current (A)	Power (kW)	H2_in (nlpm)	H2_re (nlpm)	Flow_re (nlpm)	mole fraction		
					H2	N2	Vapor
50	13.3	103.9	177	377.8	0.468	0.415	0.116
100	25.2	207.9	257.2	510.1	0.504	0.365	0.131
150	36.4	311.9	316.4	595.4	0.531	0.326	0.143
200	47	415.8	350.1	639.2	0.548	0.308	0.144
225	52.2	467.8	364.1	653	0.558	0.3	0.142
240	55.3	499.1	376.9	664.8	0.567	0.292	0.141
300	66.9	623.9	511.8	864.1	0.592	0.272	0.135
350	76.5	728	582.4	960.8	0.606	0.267	0.127
400	85.7	832	693.8	1132.3	0.613	0.265	0.122
450	95.2	936.1	821.7	1328.8	0.618	0.265	0.117
500	103.5	1040.2	986.1	1594.1	0.619	0.265	0.116

The volumetric flow rates of new and circulating hydrogen in Table 1 were converted to mass flow rates using the following conversion equations:

$$Q_m = \frac{Q_v \times \rho}{60} \quad (1)$$

Where Q_m is the mass flow rate of gas (g/s), Q_v is the volume flow rate of gas (lpm), and ρ is the density of gas (kg/m3). According to the test data of the actual gas volume flow rate and mass flow rate of the fuel cell system, the density of hydrogen in the converted high-pressure hydrogen and circulating gas is about 0.083 kg/m3.

The mass flow rate of the circulating gas is calculated by the following formula:

$$Q_R = \frac{Q_{R_{H_2}}}{w_{H_2}} \quad (2)$$

Where Q_R is the mass flow rate of circulating gas (g/s), $Q_{R\_H_2}$ is the mass flow rate of hydrogen in the circulating gas, and w_{H_2} is the mass fraction of hydrogen in the circulating gas. w_{H_2} is obtained based on the mole fraction, which is given by the following formula:

$$w_{H_2} = \frac{x_{H_2} M_{H_2}}{x_{H_2} M_{H_2} + x_{N_2} M_{N_2} + x_{H_2O} M_{H_2O}} \quad (3)$$

where x_{H_2}、x_{N_2}、x_{H_2O} are the molar fractions of hydrogen, nitrogen, and water vapor in the recycle gas, and M_{H_2}、M_{N_2}、M_{H_2O} are the molar masses of hydrogen, nitrogen, and water vapour (2 g/mol, 28 g/mol, and 18 g/mol), respectively.

The gas mass flow rate and cycle ratio demand at each current of the fuel cell were calculated according to Eqs. (1) to (3) as shown in Table 2.

Table 2 Cycle Ratio Requirements for Electric Stacks

Current(A)	H_2_in(g/s)	H_2_re(g/s)	Ration
50	0.14	3.75	26.79

100	0.29	4.85	16.72
150	0.43	5.29	12.3
200	0.58	5.39	9.29
225	0.65	5.41	8.32
240	0.69	5.43	7.87
300	0.86	6.73	7.83
350	1.01	7.33	7.26
400	1.15	8.49	7.38
450	1.29	9.93	7.7
500	1.44	11.8	8.19

2.3 Hydrogen Cycle Pressure Requirements

In fuel cell systems, the anode inlet and outlet usually have a certain pressure, which is crucial for promoting electrochemical reactions, and the pressure drop at the anode under different currents can show significant differences. Therefore, the design of the hydrogen circulation system must consider the pressure characteristics of the fuel cell under various operating conditions. The inlet and outlet pressures of the stack under each current were obtained by testing as shown in Table 3.

Table 3 Hydrogen Cycle Pressure Requirements

Current(A)	P_in(kPa)	P_out(kPa)	P_in/P_out
50	132	126	1.048
100	138	130	1.062
150	142	133	1.068
200	148	138	1.072
225	152	142	1.07
240	155	145	1.069
300	166	155	1.071
350	181	169	1.071
400	197	184	1.071
450	220	206	1.068
500	237	221	1.072

2.4 Hydrogen Circulation Pump Selection

Since the cycling performance of the elicitor is poor at small currents and the power consumed by the circulation pump increases with the increase of the rotational speed, when the combination of the elicitor and the hydrogen circulation pump is selected as the hydrogen cycling device, the elicitor is made to exert its performance at large currents while the circulation pump mainly works at small currents. Based on this, the current interval of 0~500A of the fuel cell is initially divided according to 60% of the maximum current, i.e., divided into two working intervals of 0~300A and 300~500A. When making the selection of hydrogen circulation pump, the performance of hydrogen circulation pump should at least meet the circulation demand under 0~300A. According to Tables 1 and 3, the hydrogen circulation system should be able to meet the flow rate of 377.8~864.1 lpm at a pressure ratio of less than 1.072.

Based on the requirement analysis, a hydrogen circulation pump with MAP as shown in Figure 2 was selected as follows. A single pump can circulate gas flow between 185.6~1150slpm at a pressure ratio of 1.072, which can cover the circulating demand under 0~300A.

Since the inducer performs better at high currents, it is expected that the circulating pump will only need to maintain relatively low speed operation at high currents to meet the demand. The maximum demand flow rate of the stack is 1594.1nlpm, and further considering the reliability and fault tolerance of the system, when designing the ejector, the maximum circulating gas flow rate of the ejector and the hydrogen circulation pump at a certain pressure ratio should reach 1650nlpm. at the same time, the ejector needs to overcome the anode flow resistance of the fuel cell, and the pressure ratio has to be greater than 1.072. Therefore, the secondary flow rate at a pressure ratio of 1.072 and a secondary flow rate of 1650nlpm is taken as the design target of the ejector. 1650nlpm secondary flow rate as the design goal of the pilot ejector.

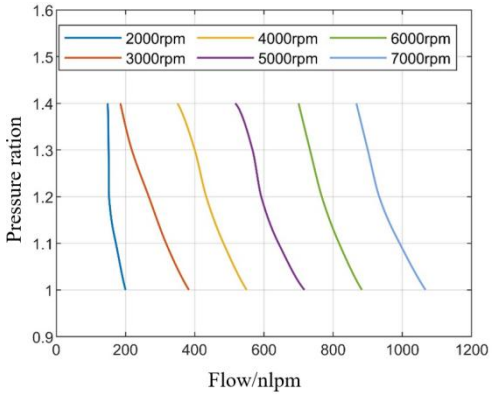

Figure 2 MAP Diagram of a Certain Type of Hydrogen Circulation Pump

3 MODELLING OF KEY COMPONENTS

The hydrogen recirculation system designed in this paper has two key components, which are the inducer and the hydrogen recirculation pump. In order to study the arrangement scheme and matching control strategy of the ejector and the hydrogen circulation pump, one-dimensional modelling of the ejector and the hydrogen circulation pump is carried out.

3.1 Ejector

The one-dimensional modelling of the ejector is carried out based on the one-dimensional gas dynamics of compressible gases, and the flow characteristics of the fluid are solved by applying the equations of conservation of mass, conservation of momentum, and conservation of energy. When the structural parameters of the ejector are known, its performance can be evaluated by the one-dimensional model, which calculates the flow characteristics of the fluid in the primary flow inlet, the inhalation chamber, the secondary flow inlet, the mixing chamber, and the diffusion chamber in turn according to the axial position, and then calculates the ejection ratio. In addition, when designing the ejector, the ejector 1D model is also capable of outputting structural parameters from the performance parameters.
The one-dimensional model of the pilot is based on the following assumptions:
(1) The gases are all ideal gases;
(2) The velocity of the primary flow is uniform in the radial direction;
(3) The internal walls of the inducer are adiabatic;
(4) The calculation of friction losses is isentropic.

3.1.1 Primary flow

When the primary flow flows from the inlet to the nozzle outlet, the flow velocity and pressure characteristics of the gas vary greatly according to Bernoulli's principle. The flow velocity at the outlet of the constricted nozzle is classified into sonic and subsonic flow according to the critical value v_{cr} of the ratio of the pressure of the secondary flow to the primary flow, P_s/P_p, as shown in Figure 3. When the pressure ratio is less than the critical value v_{cr}, the fluid flow rate does not follow the pressure ratio, while when the pressure ratio is greater than the critical value v_{cr}, the fluid flow rate decreases with the increase of the pressure ratio.

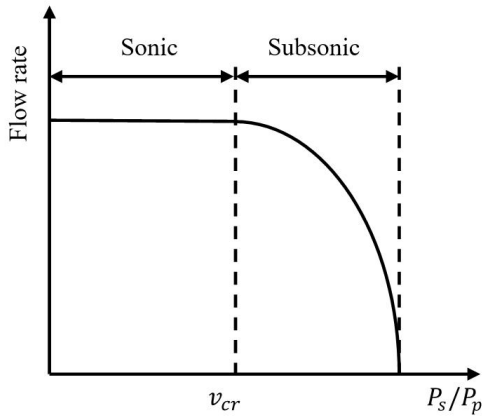

Figure 3 Flow Characteristics at the Outlet of a Shrinkage Nozzle

In this case, the formula for calculating the critical value is as follows:

$$v_{cr} = \left(\frac{2}{k_p+1}\right)^{\frac{k_p}{k_p-1}} \tag{4}$$

Where, k_p is the gas adiabatic index, which is taken as k_p=1.41 since the primary stream of the inducer is pure hydrogen, which is a diatomic molecule.

The flow characteristics from the primary flow inlet to the nozzle outlet are calculated according to the isentropic flow law to obtain the mass flow rate and Mach number at the primary flow nozzle outlet. Where Mach number is the ratio of the fluid velocity to the speed of sound in its surrounding medium.

1) For $\frac{P_s}{P_p} < v_{cr}$, the fluid is in acoustic flow, and the primary flow rate and outlet Mach number are:

$$m'_{p,0} = A_t P_{p,0} \sqrt{\frac{\Psi_{p,0} k_p}{R_{g,p} T_{p,0}}} \left(\frac{2}{k_p+1}\right)^{\frac{k_p+1}{2(k_p-1)}} \tag{5}$$

$$M_t = 1 \tag{6}$$

2)For $\frac{P_s}{P_p} \geq v_{cr}$, the fluid is in subsonic flow, and the primary flow rate and outlet Mach number are:

$$m'_{p,0} = A_t P_{p,0} \sqrt{\frac{2\psi_p k_p \left[\left(\frac{P_{s,0}}{P_{p,0}}\right)^{\frac{2}{k_p}} - \left(\frac{P_{s,0}}{P_{p,0}}\right)^{\frac{k_p+1}{k_p}}\right]}{(k_p-1) R_{g,p} T_{p,0}}} \tag{7}$$

$$M_t = \sqrt{\frac{2\left[1-\left(\frac{P_{s,0}}{P_{p,0}}\right)^{\frac{k_p-1}{k_p}}\right]}{k_p-1}} \tag{8}$$

where subscripts 0 and t denote the fluid properties at the inlet of the primary or secondary flow and at the outlet of the nozzle, respectively, subscripts p and s denote the primary and secondary flow, respectively, m is the mass flow rate (kg/s), M is the Mach number, A is the cross-sectional area (m2), P is the pressure (Pa), ψ is the isentropic coefficient considering friction losses, Rg is the gas constant (J/(kg·K)), and T is the temperature (K).

In order to improve the accuracy of the model, the primary flow rate was corrected according to the experimental data, and the corrected formula was:

$$m_{p,0} = \begin{cases} 1.6m'_{p,0} & P_{p,0} \leq 100\text{kPa} \\ 1.2m'_{p,0} & 100\text{kPa} < P_{p,0} \leq 300\text{kPa} \\ m'_{p,0} & 300\text{kPa} < P_{p,0} \leq 600\text{kPa} \\ 0.92m'_{p,0} & 600\text{kPa} < P_{p,0} \leq 800\text{kPa} \\ 0.91m'_{p,0} & P_{p,0} > 800\text{kPa} \end{cases} \tag{9}$$

3.1.2 Inhalation chamber

The one-dimensional model of a conventional ejector assumes that the pressure in the inhalation chamber is equal to the secondary inflow pressure, however, the pressure of the primary flow from the nozzle outlet to the inhalation chamber decreases, and the pressure difference with the secondary flow pressure causes the secondary flow to be sucked in. In order to improve the accuracy of the model, the formula for the pressure in the inhalation chamber in this paper adopts the modified formula in the literature [14]:

$$P_{p,2} = \begin{cases} 0.957P_{s,0} & (P_{p,0} \leq 125\text{kPa}) \\ 0.895P_{s,0} & (125\text{kPa} < P_{p,0} \leq 150\text{kPa}) \\ 0.845P_{s,0} & (150\text{kPa} < P_{p,0} \leq 175\text{kPa}) \\ 0.795P_{s,0} & (175\text{kPa} < P_{p,0} \leq 200\text{kPa}) \\ 0.690P_{s,0} & (200\text{kPa} < P_{p,0} \leq 250\text{kPa}) \\ 0.570P_{s,0} & (250\text{kPa} < P_{p,0} \leq 300\text{kPa}) \\ 0.470P_{s,0} & (300\text{kPa} < P_{p,0} \leq 400\text{kPa}) \\ 0.400P_{s,0} & (400\text{kPa} > P_{p,0}) \end{cases} \tag{10}$$

where the subscript 2 indicates the flow characteristics of the fluid at the inlet of the mixing chamber.

Based on this, the flow characteristics of the primary flow at cross-section 2 are calculated by assuming that the primary flow has a constant velocity over a certain range at cross-section 2 according to the isentropic flow law and the law of conservation of energy:

$$M_{p,2} = \sqrt{\frac{2\left(\frac{P_{p,0}}{P_{s,0}}\right)^{\frac{k_p-1}{k_p}} - 2}{k_p-1}} \tag{11}$$

$$T_{p,2} = \frac{T_{p,0}}{1+\frac{1}{2}(k_p-1)M_{p,2}^2} \tag{12}$$

$$V_{p,2} = M_{p,2}\sqrt{k_p R_{g,p} T_{p,2}} \tag{13}$$

$$D_{p,2} = \frac{D_t}{\Psi_{exp}}\sqrt{\frac{M_t}{M_{p,2}}}\left[\frac{2+(k_p-1)M_{p,2}^2}{2+(k_p-1)M_t^2}\right]^{\frac{k_p+1}{4(k_p-1)}} \tag{14}$$

Where V denotes the fluid velocity (m/s), D is the cross-sectional diameter (m), and Ψ_{exp} is the coefficient of friction loss at the beginning of mixing of the primary and secondary flows.

3.1.3 Secondary flow

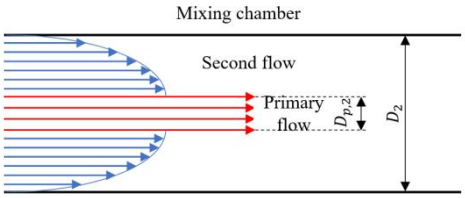

Figure 4 Schematic of the Velocity Distribution at the Entrance to the Mixing Chamber of the Inducer

The secondary flow is distributed outside the primary flow as it flows to the inlet 4 of the mixing chamber, and its velocity is not uniform in the radial direction, as shown in Figure 4. The primary flow is within $D_{p,2}$, while the secondary flow is predominant within the mixing chamber beyond $D_{p,2}$.The velocity function at the inlet of the mixing chamber with respect to primary and secondary flow is defined as [15]:

$$v_r = \begin{cases} V_{p,2} & ,\ 0 \le r \le R_{p,2} \\ V_{p,2}\left(\frac{R_2-r}{R_2}\right)^{\frac{1}{n_v}}, & R_{p,2} \le r \le R_2 \end{cases} \tag{15}$$

Where R is the cross-section radius (m), n_v is the velocity coefficient, a parameter related to the nozzle outlet diameter, mixing chamber diameter, primary and secondary flow pressure, which can be calculated by empirical formula:

$$n_v = 1.393 \times 10^{-4} e^{\frac{\beta_p}{0.05}} + 0.456\beta_D + 0.1668 \tag{16}$$

Where β_P is a pressure parameter and β_D is a structural parameter calculated as follows:

$$\beta_P = \frac{p_s^{0.8}}{p_p^{1.1}} \tag{17}$$

$$\beta_D = \frac{D_2}{D_t} \tag{18}$$

Based on the velocity function, the secondary flow rate at the inlet of the mixing chamber is calculated by the following equation:

$$m_{s,2} = \int_{R_{p,2}}^{R_2} \overline{\rho_{s,0}} v_r dA_2 \tag{19}$$

where $\overline{\rho_{s,0}}$ is the average density of the secondary stream (kg/m3), which can be calculated from the ideal gas equation of state. The mass fraction of nitrogen and water vapour is first calculated from the mass fraction of hydrogen in the secondary stream:

$$w_{N_2} = \frac{x_{N_2} M_{N_2}}{x_{H_2} M_{H_2} + x_{N_2} M_{N_2} + x_{H_2O} M_{H_2O}} \tag{20}$$

$$w_{H_2O} = \frac{x_{H_2O} M_{H_2O}}{x_{H_2} M_{H_2} + x_{N_2} M_{N_2} + x_{H_2O} M_{H_2O}} \tag{21}$$

Then, the average density of the secondary flow gas is calculated from the ideal gas equation of state as follows:

$$\overline{\rho_{s,0}} = \frac{P_{s,0}}{R_u T_{s,0}}\left(M_{H_2} \cdot w_{N_2} + M_{N_2} \cdot w_{N_2} + M_{H_2O} \cdot w_{H_2O}\right) \tag{22}$$

where R_u is the molar gas constant (J/(mol·K)).

Mass flow rate of the secondary flow at the inlet of the mixing chamber:

$$m_{s,2} = 2\pi V_{p,2}\overline{\rho_{s,0}}\left[\frac{n_v R_2^2}{n_v+1}\left(1-\frac{R_{p,2}}{R_2}\right)^{\frac{n_v+1}{n_v}} - \frac{n_v R_2^2}{2n_v+1}\left(1-\frac{R_{p,2}}{R_2}\right)^{\frac{2n_v+1}{n_v}}\right] \tag{23}$$

At this point, both the primary and secondary flow rates are known, and the priming ratio can be calculated by the following equation:

$$\lambda = \frac{m_{s,2}}{m_{p,0}} \tag{24}$$

Calculate the average velocity of the secondary flow at the inlet of the mixing chamber:

$$V_{s,2} = \frac{m_{s,2}}{\overline{\rho_{s,0}} A_{s,2}} = \frac{2\pi V_{p,2}}{A_{s,2}}\left[\frac{n_v R_2^2}{n_v+1}\left(1-\frac{R_{p,2}}{R_2}\right)^{\frac{n_v+1}{n_v}} - \frac{n_v R_2^2}{2n_v+1}\left(1-\frac{R_{p,2}}{R_2}\right)^{\frac{2n_v+1}{n_v}}\right] \tag{25}$$

where $A_{s,2}$ is the cross-sectional area of the flow region of the secondary flow at the inlet of the mixing chamber, calculated as:

$$A_{s,2} = \pi\left(R_2^2 - R_{p,2}^2\right) \tag{26}$$

The Mach number, pressure and temperature of the secondary flow at the inlet of the mixing chamber are calculated by the following equation:

$$M_{s,2} = \frac{V_{s,2}}{\sqrt{k_s R_{g,s} T_s}} \tag{27}$$

$$P_{s,2} = \frac{P_{s,0}}{\left(1+\frac{k_s-1}{2}M_{s,2}^2\right)^{\frac{k_s}{k_s-1}}} \tag{28}$$

$$T_{s,2} = \frac{T_s}{1+\frac{1}{2}(k_s-1)M_{s,2}^2} \tag{29}$$

where k_s is the gas adiabatic index of the secondary flow of the inducer. Since the model assumes that the secondary flow is an ideal gas, k_s is equal to the specific heat ratio, which is calculated as follows [16]:

$$k_s = k_{H_2} w_{N_2} + k_{N_2} w_{N_2} + k_{H_2O} w_{N_2O} \tag{30}$$

Where k_{H_2}、k_{N_2}、k_{H_2O} are the specific heat ratios of hydrogen, nitrogen, and water vapour, respectively.

3.1.4 Mixing chambers

In the process of mixing primary and secondary flow in the mixing chamber, the fluid velocity, temperature and pressure can be calculated by the equations of conservation of momentum, conservation of energy and conservation of mass, and the fluid characteristics at the outlet of the mixing chamber are calculated as follows:

$$V_3 = \frac{\Psi_{mix}(m_{p,0}V_{p,2}+m_{s,2}V_{s,2})}{m_{p,0}+m_{s,2}} \tag{31}$$

$$T_3 = \frac{1}{Cp_{mix}}\left[\frac{m_{p,0}\left(Cp_{p,2}T_{p,2}+\frac{V_{p,2}^2}{2}\right)+m_{s,2}\left(Cp_{s,2}T_{s,2}+\frac{V_{s,2}^2}{2}\right)}{m_{p,0}+m_{s,2}} - \frac{V_3^2}{2}\right] \tag{32}$$

$$P_3 = \frac{(m_{p,0}+m_{s,2})\cdot R_{g,mix}T_3}{V_3 A_3} \tag{33}$$

Where Ψ_{mix} is the friction loss coefficient for mixing primary and secondary flows in the mixing chamber, Cp_{mix} is the constant pressure specific heat capacity of the gas mixture (J/(kg·K)), and $R_{g,mix}$ is the gas constant of the gas mixture (J/(kg·K)). Cp_{mix} is calculated using the following formula:

$$Cp_{mix} = Cp_{H_2} w'_{H_2} + Cp_{N_2} w'_{N_2} + Cp_{H_2O} w'_{H_2O} \tag{34}$$

where Cp_{H_2}、Cp_{N_2}、Cp_{H_2O} are the constant pressure specific heat capacity of hydrogen, nitrogen, and water vapour (J/(kg·K)), respectively, and w'_{H_2}、w'_{N_2}、w'_{H_2O} are the mass fractions of hydrogen, nitrogen, and water vapour in the gases mixed in the primary and secondary streams, respectively.

The Mach number of the gas at the exit of the mixing chamber is:

$$M_3 = \frac{V_3}{\sqrt{k_3 R_{g,mix} T_3}} \tag{35}$$

where k_3 is the gas adiabatic index of the secondary flow of the inducer, calculated in the same way as k_s.

3.1.5 Diffusion chambers

The flow of the gas mixture in the diffusion chamber is a decreasing velocity and increasing pressure process, and the pressure at the outlet of the inducer is calculated by the isentropic flow law:

$$P_4 = P_3\left[1+\frac{1}{2}(k_3-1)M_3^2\right]^{\frac{k_3}{k_3-1}} \tag{36}$$

The temperature at the exit of the ejector is calculated according to the law of conservation of energy from the inlet to the outlet of the ejector:

$$T_4 = \frac{m_p Cp_{H_2} T_p + \left(m_{s,H_2}Cp_{H_2}+m_{s,N_2}Cp_{N_2}+m_{s,H_2O}Cp_{H_2O}\right)T_s - E_{loss}}{\left(m_p+m_{s,H_2}+m_{s,N_2}+m_{s,H_2O}\right)*Cp_{mix}} \tag{37}$$

Where E_{loss} is the energy loss (J/s) of primary and secondary flow, which is calculated as follows:

$$E_{loss} = \frac{1}{2}(1-\Psi_p)m_p V_{p,2}^2 + \frac{1}{2}(1-\Psi_s)m_s V_{s,2}^2 \tag{38}$$

3.1.6 Validation of the elicitor model

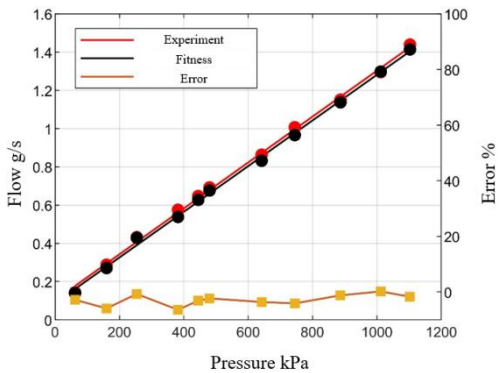

Figure 5 Validation of the Model of the Introducer

In order to verify the accuracy of the pilot model, this paper simulates the pilot and derives the experimental data under the same boundary conditions as the simulation. By fitting the experimental and simulation data and calculating the relative error, the results are shown in Figure 5. It can be seen that the simulation and experimental results of the primary flow rate have the same trend, and the relative error of the two is between -6.4% and 0.2%, which can be concluded that the pilot model established in this paper has high accuracy and can be used for subsequent research.

3.2 Hydrogen Circulation Pumps

The one-dimensional model of the hydrogen circulation pump consists of three sub-models, namely the flow-pressure ratio relationship model, the torque and angular velocity model of the drive motor, and the PID control model of the motor.

3.2.1 Flow-pressure ratio model

The flow-pressure ratio relationship model of the hydrogen circulating pump is based on the test data and established by the method of checking the table. The model takes the component partial pressures of the inlet and outlet gases of the circulating pump and the rotational speed of the circulating pump as input parameters, and can output the circulating pump outlet gas flow rate and the amount of power loss.

3.2.2 Torque and angular velocity modelling of the drive motor

The torque and angular velocity model of the hydrogen circulating pump motor is based on the following equations:

$$\frac{d\omega_l}{dt} = \frac{1}{J_l}(\tau_m - \tau_l) \tag{39}$$

where the subscripts l and m denote the load and drive motor parameters, respectively, ω is the angular velocity of the rotor (rad/s); t is the time (s); J is the rotational moment of inertia of the rotor of the hydrogen circulating pump (kg·m2); and τ is the torque (N·m). Among them, the driving torque and load torque are calculated by the following equation:

$$\tau_m = \eta_m \frac{\kappa_t}{R_m}(u_m - \kappa_v \omega_l) \tag{40}$$

$$\tau_l = \frac{P_l}{\omega_l} \tag{41}$$

Where η is the efficiency; R_m is the motor resistance (Ω); κ_t、κ_v denote the torque constant and voltage constant of the motor, respectively; u_m denotes the motor control voltage (V). P_l is the power consumed by the hydrogen circulation pump, which is calculated by the following formula:

$$P_l = Cp_{in}\frac{T_{in}}{\eta_l}\left[\left(\frac{P_{out}}{P_{in}}\right)^{\frac{k_{in}-1}{k_{in}}} - 1\right] m_{in} \tag{42}$$

Where Cp_{in} is the constant-pressure specific heat capacity of the inlet gas of the circulating pump (J/(kg·K)); T_{in} is the temperature of the inlet gas (K); P_{out}、P_{in} represent the pressures of the outlet and the inlet, respectively (Pa); k_{in} is the specific heat ratio of the inlet gas; and m_{in} is the mass flow rate of the inlet gas (kg/s).

The formula for calculating the outlet gas temperature of a hydrogen circulation pump is as follows:

$$T_{out} = T_{in} + \frac{T_{in}}{\eta_l}\left[\left(\frac{P_{out}}{P_{in}}\right)^{\frac{k_{in}-1}{k_{in}}} - 1\right] \tag{43}$$

Where T_{out} is the circulating pump outlet temperature (K).

3.2.3 PID control model for motors

In the hydrogen circulation system, the proportional valve serves to control the inlet pressure, and the speed of the hydrogen circulation pump has a significant effect on the circulation system flow and pressure, therefore, precise control of the circulation pump is required.

When the circulating pump speed is stable, its control voltage is calculated by means of the angular velocity, which is calculated as follows:

$$u_m = \kappa_v \omega_l + \frac{P_l R_m}{\omega_l \eta_m \kappa_t} \tag{44}$$

Calculate the amount of deviation of the actual angular velocity from the target angular velocity:

$$e(t) = \omega_{set} - \omega_l \tag{45}$$

where ω_{set} is the target angular velocity (rad/s) and e(t) is the angular velocity deviation (rad/s).

The deviation amount of angular velocity, e(t), is used as an input to the PID to calculate the control voltage after control:

$$u(t) = K_P e(t) + K_I \int e(t)dt + K_D \frac{de(t)}{dt} \tag{46}$$

$$u_{m,new} = u_m + u(t) \tag{47}$$

Where, K_P、K_I、K_D represent proportional, integral and differential coefficients, respectively; u(t) is the change of control voltage (V); $v_{m,new}$ is the control voltage (V) after PID control.

Set the PID coefficients as $K_P = K_I = K_D = 1$, the rotational speed of circulating pump is correspondingly as shown in Fig. 2.7(a), and the deviation from the target rotational speed is large. Adjust the PID parameters to $K_P = 150$, $K_I = 5$, $K_D = 100$, the control effect is shown in Figure 6, the circulating pump speed to reach the target speed of the time is greatly shortened, to achieve efficient control.

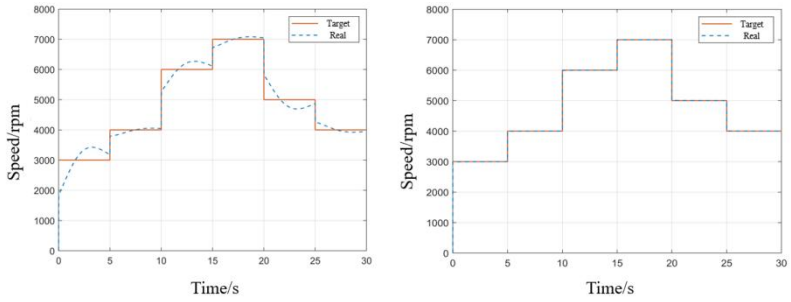

Figure 6 PID Control Effect of Hydrogen Circulating Pump

3.2.4 Hydrogen circulation pump model validation

In order to verify the accuracy of the hydrogen circulating pump model, a set of data was randomly selected for simulation and compared with the experimental results. During the simulation process, the inlet pressure of the circulating pump is set at 100 kPa and the rotational speed is 6000 rpm, and the comparison between the obtained volume flow rate simulation data and the experimental data is shown in Figure 7. The maximum relative error between the simulation data and experimental data is 0.82%, and it can be concluded that the accuracy of the established circulation pump model is high.

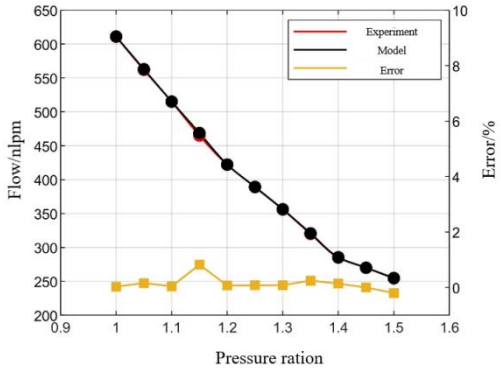

Figure 7 Hydrogen Circulation Pump Model Validation

4 MATCHING CONTROL STRATEGY FOR HYDROGEN CIRCULATION SYSTEM

4.1 Ejector in Series with a Hydrogen Circulation Pump

When the ejector is connected in series with the hydrogen circulation pump, the gas at the outlet of the circulation pump is used as the secondary flow of the ejector, and the sum of the pressures of the ejector and the circulation pump is equal to the anode flow resistance of the fuel cell.

In the state where the ejector and the hydrogen circulation pump are connected in series, they share the responsibility of overcoming the flow resistance of the fuel cell anode. Based on the pressure requirement of the fuel cell anode, the minimum pressure rise of the hydrogen circulation pump can be calculated by the following equation:

$$\Delta P_{pump} = \Delta P_{anode} - \Delta P_{ejector} \tag{48}$$

Since the ejector and the hydrogen circulation pump are connected in series, they share the pressure of the anode, and in order to ensure the circulating flow of the hydrogen circulation system, the hydrogen circulation pump has to be operated continuously over the entire current range. Therefore, it is necessary to carry out a reasonable pressure distribution between the ejector and the hydrogen circulation pump. On the one hand, when the circulating pump speed is certain, the pressure rise of the circulating pump should be made lower to ensure more circulating gas volume, so that the elicitor should share as much pressure as possible; on the other hand, under the premise of satisfying the circulating volume, the circulating pump speed should be set smaller in order to reduce the power consumption (Figure 8).

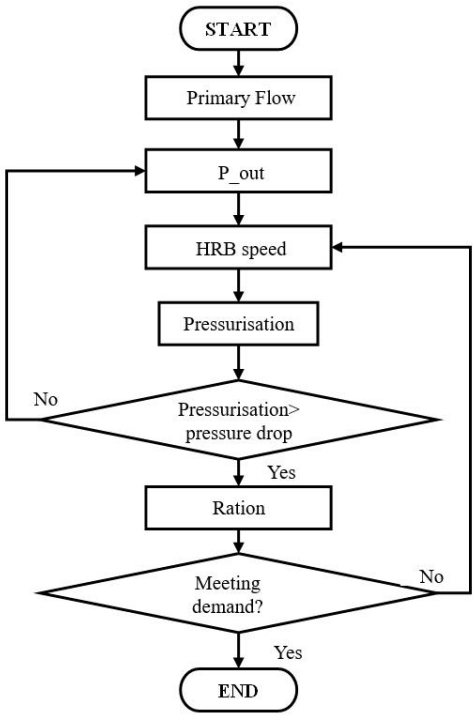

Figure 8 Flow of Formulation of Matching Strategy in the Cascade Mode of Inducer and Hydrogen Recirculation Pump

4.2 Parallel Connection of the Ejector and the Hydrogen Circulation Pump

The characteristics of pilot and hydrogen circulating pump in parallel are 'equal pressure rise, divided flow', that is, the pressure rise of both is equal to the anode pressure drop, and the circulating flow is shared by both.

In the current range of 100A and below, the injector can not overcome the anode flow resistance of the fuel cell, and then the phenomenon of secondary flow reversal may occur, which may lead to a significant reduction in the cycle efficiency, and even affect the normal operation of the fuel cell. In order to avoid the occurrence of reverse flow phenomenon, this paper adds a check valve in the secondary flow gas flow path of the ejector. After adding the check valve, the backflow phenomenon of the secondary flow was alleviated, but it also resulted in almost no circulating gas entering the elicitor. Therefore, the hydrogen recirculation pump is considered to work alone in the current range of 100 A and below (See Figure 9).

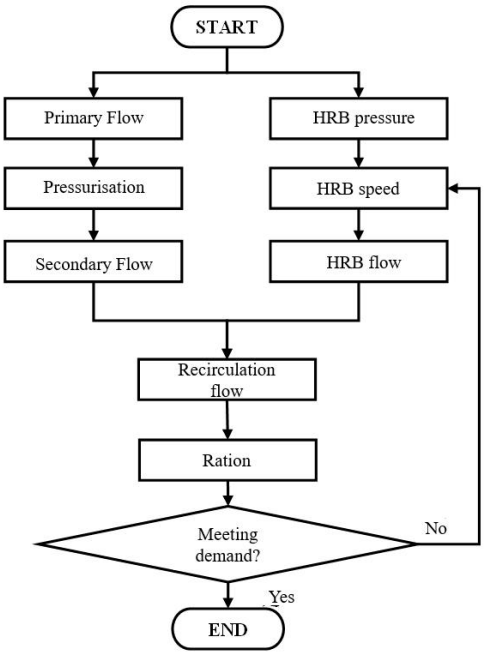

Figure 9 Flow of Formulation of Matching Strategy in Parallel Mode of Inducer and Hydrogen Circulating Pumps

The matching strategies of the pilot and the hydrogen circulation pump under two arrangement schemes, series and parallel, have been developed in the previous section, and both arrangement schemes can meet the hydrogen circulation demand of the fuel cell system. In the series and parallel schemes, the speed of the hydrogen circulation pump at each current point is shown in Table 4, and its average power consumption is 0.42kW and 0.39kW, respectively, and the power consumption under the parallel scheme is 7.1% smaller than that of the series scheme. Therefore, it was finally determined that the arrangement scheme of the ejector and the hydrogen circulation pump was parallel connection.

Table 4 Comparison of Hydrogen Circulation Pump Speed in Different Hydrogen Circulation Modes

Current (A)	Series HRB speed (rpm)	Parallel HRB speed (rpm)
50	3000	5000
100	4000	5000
150	4000	5000
200	4000	5000
225	4000	5000
240	4000	3000
300	5000	3000
350	5000	3000
400	6000	3000
450	6000	3000
500	6000	3000

5 CONCLUSION

In this paper, the optimized design of the hydrogen circulation system is carried out for automotive fuel cell systems. For the fuel cell electric stack, the flow rate and pressure demand of the circulation device design are analysed, the demand allocation for the elicitor and the hydrogen circulation pump is carried out, and the model of the hydrogen circulation pump is determined.

According to the one-dimensional design theory of the ejector, a one-dimensional model of the ejector is established; based on the experimental data of the hydrogen circulation pump, its one-dimensional model is established. Based on the experimental data, the one-dimensional model is verified to ensure the accuracy of the model.

Finally, based on the one-dimensional model of the ejector and the hydrogen circulation pump, the pressure rise or flow rate of the ejector and the hydrogen circulation pump in series and parallel are calculated, and the matching strategy is formulated. By comparing the power consumption under the series and parallel schemes, it is found that the average power consumption under the parallel scheme is 7.1% smaller than that of the series, so the parallel scheme is selected.

COMPETING INTERESTS

The authors have no relevant financial or non-financial interests to disclose.

FUNDING

This work was supported by China National Railway Group Co., Ltd. Unveiled Its Flagship Project (grant number: N2022J016-A) and Changzhou City's "Unveiling the List and Leading the Way" Science and Technology Research Project (grant number: 2023-Z-GKB-JS-0009).

REFERENCES

[1] Mohsen Kandi Dayeni, Mehdi Soleymani. Intelligent energy management of a fuel cell vehicle based on traffic condition recognition. Clean Technologies and Environmental Policy, 2016, 18(6): 1945-1960.
[2] Zhu Mengqian, Xie Xu, Wu Kangcheng, et al. Experimental investigation of the effect of membrane water content on PEM fuel cell cold start. Energy Procedia, 2019, 158: 1724-1729.
[3] Kairui Dong, Guangbin Liu. A review of hydrogen recirculation systems for fuel cells. Power Technology, 2021, 45(04): 545-551.
[4] Zhangming Zhang. Design of Hydrogen Cycle Subsystem for High Power Fuel Cells. Tongji University, 2021.
[5] Zhang L X, Li J, Li R Y, et al. A review of hydrogen supply system for automotive fuel cells. Journal of Engineering Thermophysics, 2022, 43(06): 1444-1459.
[6] Tsai ShangWen, Chen YongSong. A mathematical model to study the energy efficiency of a proton exchange membrane fuel cell with a dead-ended anode. Applied Energy, 2017, 188: 151-159.

[7] Bao Cheng, Ouyang Minggao, Yi Baolian. Modeling and control of air stream and hydrogen flow with recirculation in a PEM fuel cell system—I. Control-oriented modeling. International Journal of Hydrogen Energy, 2006, 31(13): 1879-1896.
[8] Mohsen Dadvar, Ebrahim Afshari. Analysis of design parameters in anodic recirculation system based on ejector technology for PEM fuel cells: A new approach in designing. International Journal of Hydrogen Energy, 2014, 39(23): 12061-12073.
[9] Ma Tiancai, Cong Ming, Meng Yixun, et al. Numerical studies on ejector in proton exchange membrane fuel cell system with anodic gas state parameters as design boundary. International Journal of Hydrogen Energy, 2021, 46(78): 38841-38853.
[10] Shen YiWei. Characterisation of a rotary vortex hydrogen circulating pump. China University of Petroleum (Beijing), 2023.
[11] He Lingxuan. Thermodynamic Analysis and Comprehensive Evaluation of Vehicle Fuel Cell Power System under Dynamic Operating Conditions. Hunan Institute of Science and Technology, 2023.
[12] Wang Miao. Simulation and control strategy of hydrogen supply system for fuel cell engine. Shandong University,2023. Barbir F. PEM Fuel Cells: Theory and Practice. Burlington: Elsevier/Academic Press, 2005.
[13] Zhang DengHao. Influence of structural and operating parameters of a primer on the priming ratio. Donghua University, 2023.
[14] Yinhai Zhu, Yanzhong Li. New theoretical model for convergent nozzle ejector in the proton exchange membrane fuel cell system. Journal of Power Sources, 2009, 191(2): 510-519.
[15] Yang Z J. Deep learning-based dynamic modelling of automotive proton exchange membrane fuel cells. Tianjin University, 2022.